Published in final edited form as:
J Neuropathol Exp Neurol. 2012 November ; 71(11): 1018–1029. doi:10.1097/NEN.0b013e318272caab.

Hippocampal ProNGF Signaling Pathways and β-Amyloid Levels in Mild Cognitive Impairment and Alzheimer Disease

Elliott J. Mufson, PhD[1], **Bin He, MD**[1], **Muhammad Nadeem, MD**[1], **Sylvia E. Perez, PhD**[1], **Scott E. Counts, PhD**[1], **Sue Leurgans, PhD**[2], **Jason Fritz, PhD**[3], **James Lah, MD**[3], **Stephen D. Ginsberg, PhD**[4], **Joanne Wuu, MS**[5], and **Stephen W. Scheff, PhD**[6]

[1]Department of Neurological Science, Rush University Medical Center, Chicago, Illinois

[2]Rush Alzheimer's Disease Center, Chicago, Illinois

[3]Center for Neurodegenerative Disease and Department of Neurology, Emory University, Atlanta, Georgia

[4]Center for Dementia Research, Nathan Kline Institute, Orangeburg, New York, and Departments of Psychiatry, and Physiology & Neuroscience, New York University Langone Medical Center, New York, New York

[5]Department of Neurology, University of Miami Miller School of Medicine, Miami, Florida

[6]Sanders-Brown Center on Aging, University Kentucky College of Medicine, Lexington, Kentucky

Abstract

Hippocampal precursor of nerve growth factor (proNGF)/NGF signaling occurs in conjunction with β-amyloid (Aβ) accumulations in Alzheimer disease (AD). To assess the involvement of this pathway in AD progression, we quantified these proteins and their downstream pathway activators in postmortem tissues from the brains of subjects with no cognitive impairment (NCI), mild cognitive impairment (MCI), and AD using immunoblotting and enzyme-linked immunosorbent assay (ELISA). Hippocampal proNGF was significantly greater in AD compared to NCI and MCI cases. TrkA was significantly reduced in MCI compared to NCI and AD, whereas $p75^{NTR}$, sortilin, and neurotrophin receptor homolog-2 remained stable. Akt decreased from NCI to MCI to AD, whereas phospho-Akt and phosphor-Akt to Akt ratio were elevated in AD compared to MCI and NCI. No differences were found in phospho-Erk, Erk or their ratio across groups. c-jun kinase (JNK) remained stable across groups, while phospho-JNK and the phospho-JNK to JNK ratio increased significantly in AD compared to NCI and MCI. Expression levels of $A\beta_{1\text{-}40}$, $A\beta_{1\text{-}42}$ and $A\beta_{40/42}$ ratio were stable. Statistical analysis revealed a strong positive correlation between proNGF and phospho-JNK, though only proNGF was negatively correlated with cognitive function and only TrkA was negatively associated with pathologic criteria. These findings suggest that alterations in the hippocampal NGF signaling pathway in MCI and AD favor proNGF-mediated pro-apoptotic pathways, and that this is independent of Aβ accumulation during AD progression.

Send correspondence and reprint requests to: Elliott J. Mufson, PhD, Professor of Neurological Sciences, Alla and Solomon Jesmer Chair in Aging, Rush University Medical Center, 1735 W. Harrison Street, Suite 300, Chicago, IL 60612. Tel: 312-563-3558; Fax: 312-563-3571; emufson@rush.edu.

Keywords

Alzheimer disease; Amyloid; Mild cognitive impairment; Nerve growth factor; proNGF; Protein kinases, TrkA

INTRODUCTION

The hippocampus, a critical node of the episodic memory network, is one of the first brain sites to develop neurodegenerative changes in living individuals at risk for dementia as well as those with a clinical diagnosis of mild cognitive impairment (MCI), a prodromal stage of Alzheimer disease (AD), or AD (1, 2). Despite the expression of early degenerative events, the hippocampus displays remarkable evidence for neuroplasticity during the prodromal phase(s) of AD. For example, the activity of choline acetyltransferase, the rate-limiting enzyme for acetylcholine synthesis, is increased in the hippocampus of people with MCI (3, 4), suggesting that this region is resilient to the stress of disease onset via increased input from cholinergic neurons of the septal/diagonal band. Because damage to this pathway plays a key role in memory and attentional dysfunction during AD progression (5-7), understanding the signaling events that underlie septohippocampal plasticity are crucial for delineating the mechanisms that cause reactive synaptogenesis in this region and may provide translational information for the development of novel treatment strategies to promote cholinergic neuroplasticity over the extent of AD.

A central concept underlying the integrity of the cholinergic septohippocampal projection system is the observation that mature nerve growth factor (NGF), its pro form (proNGF) (8), and their cognate receptors play a crucial role in the function of this pathway and that their dysregulation contributes to degeneration of this projection system in AD (7). Mature NGF binds primarily to the TrkA receptor, which stimulates survival signal transduction pathways (5, 9). However, the binding of p75 neurotrophin receptor ($p75^{NTR}$) to proNGF has multiple functions including pro-apoptotic and/or cell death actions (10), which are dependent upon its interaction with co-receptor chaperones including sortilin and neurotrophin receptor homolog-2 (NRH2) (8, 10-14). NGF/proNGF receptor binding activates downstream protein kinase signaling pathways involved in pro-cell survival and pro-cell death actions (15-18) including Erk and protein kinaseB/Akt (which activate intracellular events responsible for neuronal survival and neurite differentiation [16, 19]), as well as the c-jun kinase (JNK)-mediated pro-apoptotic pathway (20). Although data suggest a close relationship between β-amyloid (Aβ) and NGF receptor signaling in AD (21, 22), it remains to be determined whether alterations in hippocampal proNGF signaling track with changes in Aβ levels during the onset of AD. In fact, the majority of studies on proNGF/NGF signaling have been performed on cellular or animal models of cerebral amyloid overexpression, not on bona fide human AD brain tissues.

To characterize whether AD disease progression affects the expression level of these cell survival and pro-apoptotic pathways within the hippocampus relative to Aβ deposition, (23), we examined tissue harvested from people who died with a premortem clinical diagnosis of no cognitive impairment (NCI), MCI or AD using Western blot and ELISA technology and correlated these findings with cognitive and neuropathologic variables.

MATERIALS AND METHODS

Subjects

This study included 37 cases with an antemortem clinical diagnoses of NCI (n = 11, 6F/5M, mean age at death ± SD = 83.4 ± 4.6 years, Mini-Mental State Examination [MMSE] 27.6 ±

1.4), MCI (n = 13, 8F/5M, 85.4 ± 4.0 years, MMSE 27.5 ± 2.5) and AD (n = 13, 7F/6M, 87.7 ± 5.8 years, MMSE 19.9 ± 6.4) from the Rush Religious Order Study (RROS) (Table 1) (24-26). Each participant had agreed to an annual detailed premortem clinical evaluation and brain donation at the time of death. An additional 7 NCI (6F/1M, 83.7 ± 6.4 years, 28.3 ± 2.4), 5 MCI (3F/2M, 87.4 ± 3.9 years, MMSE 25.8 ± 3.3), and 5 AD (2F/3M, 84.8 ± 8.0 years, MMSE 13.2 ± 7.9) cases were obtained from the University of Kentucky ADC Brain Bank and used to measure NRH2 protein levels, which were only available in a subset of the RROS cases (5 NCI, 4 MCI, and 6 AD). The Human Research Committees of Rush University Medical Center and the University of Kentucky approved this study. Written informed consent for research and autopsy was obtained from study participants or their family/guardians.

Clinical and Neuropathological Evaluation

Details of the clinical evaluation and criteria for diagnosis of AD and MCI in the RROS cohort have been published elsewhere (24, 26, 27). There was an average time of ~8 months between death and the last clinical and neuropsychological evaluation, which included the MMSE and a battery of 19 cognitive tests. A Global Cognitive Score (GCS), a composite z-score that indicates overall cognitive function, was compiled from the 19 tests. An episodic memory z-score, which is more specific for hippocampal function, was also computed based on 7 of the tests. Among the RROS MCI cases, 4 were amnestic MCI, whereas all MCI cases from University of Kentucky ADC were amnestic MCI based upon a clinical dementia rating score of 0.5 (28). For both populations, a final clinical diagnosis was assigned after consensus conferences of neurologists and neuropsychologists who reviewed all relevant data and information collected. Neuropathological diagnosis was performed as previously described (24, 26, 27) and included Braak staging of neurofibrillary tangles (NFTs) (29), the NIA-Reagan criteria (30), and recommendations of the Consortium to Establish a Registry for Alzheimer's Disease (CERAD) (31). Subjects with pathological findings other than AD (e.g. stroke, Parkinson disease, Lewy body dementia) were excluded from the study. None of the cases examined was treated with anticholinesterase inhibitors. Clinical, demographic and neuropathological details of the RROS cases are presented in Table 1. Tissue and clinical information is under the protection of the Health Information Privacy Administration rules.

Tissue Samples

Hippocampal samples were dissected free of white matter at autopsy in the coronal plane at the level of lateral geniculate nucleus (which included all layers and cell types of this structure) on dry ice to prevent thawing of the tissue, and were frozen at −80°C until the time of biochemical assay. Frozen hippocampus was homogenized (150 mg/ml) on ice in phosphate-buffered saline and immediately divided into 2 aliquots. One aliquot was added to a homogenization buffer (250 mM sucrose, 20 mM Tris base) containing protease inhibitors (100× protease inhibitor cocktail, cat. #8340, Sigma, St. Louis, MO) and divided into 2 aliquots: one was used for the Aβ ELISA, and the second aliquot was diluted to 10 mg tissue/ml with potassium phosphate-buffered saline, pH 7.4) for Western blotting.

Antibodies

All antibodies are commercially available and their specificity has been characterized (32-34) (Table 2). The antibodies included: proNGF polyclonal antiserum (1:50, H-20 [Santa Cruz Biotechnology, Santa Cruz, CA]); purified anti-TrkA rabbit polyclonal affinity-purified antibodies (1:100, Fitzgerald, Acton, MA); anti-NRH2 (1:1000), -sortilin (1:1000) and -$p75^{NTR}$ (1:500) obtained from Abcam (Cambridge, MA); and anti-Akt (1:1000), phospho-Akt (Ser473) (1:1000), p44/p42 MAPK (Erk1/2) (1:1000), phospho-p44/p42 MAPK (Erk1/2) (Thr202/Tyr 204) (E10) mouse monoclonal antibody (mAb) (1:2000),

SAPK/JNK (56G8) rabbit mAb (1:1000), and phospho-SAPK/JNK(Thr183/Tyr185) (81E11) rabbit mAb (1:2000) obtained from Cell Signaling Technology (Danvers, MA). The loading control β-tubulin mAb (1:4000) was from Millipore (Bedford, MA).

Quantitative Immunoblotting

Briefly, sample proteins were denatured in sodium dodecyl sulfate (SDS) loading buffer to a final concentration of 5 mg/ml. Proteins (50 μg/sample) were separated by 8%-16% or 7.5% SDS polyacrylamide gel electrophoresis (Lonza, Rockland, ME) and transferred to polyvinylidene fluoride membranes (Immobilon P; Millipore) electrophoretically as described previously (35-37). Membranes were first blocked in TBS/0.05%Tween-20/5% milk for 60 minutes at room temperature (RT) with the exception of proNGF, which was blocked in 0.5X TBS/0.05% milk for 20 minutes. Phospho-JNK, phospho-Akt and phospho-Erk were blocked in TBS/0.05%Tween-20/3% BSA for 60 minutes. Primary antibodies were added to blocking buffer. After a 60-minute incubation with primary antibodies at RT, membranes were incubated overnight at 4°C. After 3 washes in TBS/0.05% Tween-20, the membranes were incubated for 1 hour at RT with horseradish peroxidase-conjugate goat anti-mouse IgG secondary antibody (1:4000; Pierce, Rockford, IL) or horseradish peroxidase-conjugated goat-anti rabbit IgG secondary antibody (1:4000, Bio-Rad, Hercules, CA). Immunoreactive proteins were visualized by enhanced chemiluminescence (Pierce) on a Kodak Image Station 440CF (Perkin-Elmer, Wellesley, MA). Bands were quantified using Kodak 1D image analysis software. Immunoreactive signals of target proteins were normalized to β-tubulin signals for quantitative analysis. Previously, we verified by immunoblotting, Coomassie blue staining, and densitometry that β-tubulin levels were unchanged in samples from the same clinical diagnostic cohort examined in the present study (36), which is consistent with findings by other groups (38, 39). Therefore, β-tubulin levels were used as the internal control for protein loading. Each sample was analyzed 3 times in independent experiments.

Sequential Amyloid Extraction and Sandwich Enzyme-linked Immunosorbent Assay for $A\beta_{1\text{-}40}/A\beta_{1\text{-}42}$

The ELISA used for $A\beta_{1\text{-}40}/A\beta_{1\text{-}42}$ levels is a modification of a previously described procedure (34). Briefly, hippocampal homogenates were diluted to 10 mg wet weight/ml in homogenization buffer containing protease inhibitors. One mg of crude homogenate was sonicated (30 seconds at 40% Amplification with a 1/8" tapered microtip; Ultrasonic Processor, Fisher Scientific, Pittsburgh, PA) in 10% SDS (final concentration 2% SDS) and centrifuged at 4°C for 1 hour at 100,000 × *g* (Optima TLX Ultracentrifuge, Beckman-Coulter, Fullerton, CA). Supernatant was collected (SDS-soluble fraction) and the pellet was resuspended in an equal volume of 70% formic acid prepared in water and sonicated again as described above. Formic acid fractions were neutralized by 1:20 dilution in 1.0 M Tris base (pH 11.3). SDS fractions were diluted at least 1:50 and neutralized formic acid fractions were further diluted if needed in ELISA diluent buffer (50 mM Tris base, 150 mM NaCl, 0.5% NP-40, 0.5% deoxycholate, 0.1 mg/ml phenylmethylsulfonyl fluoride, protease inhibitor cocktail, pH 7.4). Fractions were stored at −80°C until ELISA and were not subjected to more than 1 freeze-thaw cycle. Sandwich ELISAs specific for human $A\beta_{1\text{-}40}$ and $A\beta_{1\text{-}42}$ species (EZBRAIN40, EZBRAIN42; EMD Millipore Corporation, Billerica, MA) were performed in duplicate to measure $A\beta_{1\text{-}40}/A\beta_{1\text{-}42}$ levels according to the manufacturer's instructions. Plates were read at 450 nm on a Spectra Max Plus plate reader (Molecular Devices, Sunnyvale, CA).

Statistical Analysis

Summary statistics were provided for each variable included in the analyses (mean ± SD, range, frequency, or percentage); β-amyloid data were transformed by taking the natural

logarithm in order to reduce data skewness. Clinical, demographic, and neuropathologic characteristics were compared across the clinically defined groups of NCI, MCI, and AD by the Kruskal-Wallis test or Fisher exact test (40), as were the Western blot protein values and ELISA values for β-amyloid. Ad hoc analyses were performed with Bonferroni-type correction for multiple comparisons. Associations between biochemical measures, demographic and clinical characteristics, and neuropathology scores were assessed by Spearman rank correlation (40). Non-parametric methods were used because they are more robust to the effect of outliers and the non-normality in the data. Additional regression analyses were performed as needed to explore the potential confounding effects of clinical variables such as age (41). Due to the large number of proteins examined in this study, factor analyses (42) as well as biological rationale were employed to guide us in our results interpretation; our focus was on the identification of consistent patterns in the data rather than individual comparisons or correlations. Statistical analyses were performed using the SAS software, version 9.2 (SAS Institute Inc). The level of statistical significance was set at 0.05 (2-sided). Results with $0.01 \leq$ p-value < 0.05 were interpreted with caution.

RESULTS

Case Demographics

The clinical diagnostic groups did not differ by age, gender, years of education, or postmortem interval (Table 1). There were more subjects with an ApoE 4 allele in the MCI (38%) and AD (31%) groups than in the NCI group (0%) (Table 1). AD cases had lower MMSE scores compared to both MCI and NCI cases ($p < 0.0001$), whereas the latter 2 groups did not differ statistically (Table 1). GCS and episodic memory z-scores were significantly lower in AD vs. MCI, and in MCI vs. NCI groups. Subjects in the different clinical diagnostic groups displayed considerable heterogeneity with respect to pathological diagnostic criteria. Pathological examination of study subjects revealed that 64% of NCI cases, 85% of MCI cases, and 92% of AD cases were classified as Braak stages III-VI. Using NIA-Reagan criteria, 45% of NCI, 62% of MCI, and 92% of AD cases were classified as intermediate to high likelihood of AD (Table 1). For CERAD diagnosis, 55% of NCI, 69% of MCI, and 100% of AD cases received a diagnosis of probable/definite AD. Statistical analysis revealed a significant difference between the NCI and AD groups for NIA-Reagan ($p = 0.042$) and CERAD ($p = 0.0076$) diagnosis, but not for Braak staging.

Hippocampal proNGF, TrkA, $p75^{NTR}$, Sortilin and NRH2 Receptor Levels

The mean hippocampal proNGF levels were significantly elevated in AD vs. NCI and MCI (by 57% and 41%, respectively; $p = 0.004$; Fig. 1A). By contrast, mean hippocampal TrkA protein levels were significantly reduced in MCI vs. NCI and AD (by 27% and 36%, respectively; $p = 0.014$; Fig. 1B). TrkA expression levels in NCI and AD were comparable. There were no significant modifications in hippocampal $p75^{NTR}$ (Fig. 1C), sortilin, or NRH2 (Fig. 1D) expression levels among the 3 clinical groups (Table 3).

Hippocampal Erk and Akt Levels

There were no significant modifications in the expression levels of hippocampal total Erk, phospho-Erk, or their ratio among the 3 clinical groups (Table 3). On the other hand, total Akt levels were reduced from NCI to MCI to AD, whereas phospho-Akt expression levels appeared to be elevated in AD (by ~33%) compared to MCI and NCI (Fig. 2A, B). The ratio of phospho-Akt to Akt was then found to be significantly increased in AD ($p = 0.036$), though only the difference between AD and MCI reached statistical significance (Fig. 2C).

Hippocampal JNK and Phospho-JNK Levels

Although total mean JNK levels remained stable across clinical groups (Table 3; Fig. 3A), phospho-JNK was significantly increased by ~55% in AD vs. NCI and MCI (Fig. 3B; $p = 0.0006$). The ratio of phospho-JNK to JNK was also similarly increased in AD vs. NCI and MCI (~55%; $p = 0.016$; Fig. 3C).

Hippocampal $A\beta_{1-40}$ and $A\beta_{1-42}$ Levels

Soluble and insoluble derived $A\beta_{1-40}$, $A\beta_{1-42}$ and their ratios remained stable across NCI, MCI and AD groups (Table 4). Analysis revealed a strong positive correlation between hippocampal proNGF and phospho-JNK protein levels (Spearman correlation, $r = 0.46$, $p = 0.0039$), and both correlated negatively with cognitive functions as measured by MMSE, GCS, and episodic memory z-score ($r = -0.45$ to -0.49 and $p = 0.0021$ to 0.0052 for proNGF, $r = -0.33$ to -0.44 and $p = 0.0072$ to 0.049 for phosphor-JNK; Fig. 4). On the other hand, there was a positive correlation between TrkA and the severity of pathology based on Braak, NIA Reagan, and CERAD scores ($r = 0.39$ to 0.43, $p = 0.0050$ to 0.011). Moreover, we determined whether protein levels for each variable examined in the present study differed between NCI cases from each cohort when grouped into those with a Braak score I-II ($n = 8$) vs. III and above ($n = 9$). Statistical analysis did not reveal differences in any of the protein levels evaluated between early and more advanced Braak stage cases (data not shown).

DISCUSSION

Prior studies suggest that mature NGF levels are unchanged in the AD hippocampus compared to aged controls (43, 44), but recent biochemical studies indicate that proNGF is the major form found in the human brain (8). Here we demonstrate a significant increase in hippocampal proNGF expression levels in AD but not in MCI. Notably, proNGF levels were not modified in the MCI hippocampus compared to its up regulation in the neocortex in MCI and AD subjects (33, 45), suggesting that cholinergic forebrain projection groups respond differently during the onset of AD. Interestingly, proNGF isolated from AD cerebral cortex has been shown to induce apoptosis in neuronal cell cultures via an interaction with the $p75^{NTR}$ receptor by a mechanism that is dependent upon γ-secretase shedding of the receptor, whereas proNGF isolated from control brain samples was not able to induce apoptosis (46). Based on the current findings, it is crucial to determine whether the biological actions of proNGF isolated from MCI brain would induce apoptosis similar to that seen in AD samples or whether it acts more like proNGF in controls.

Hippocampal proNGF Levels During Disease Progression

Although proNGF binds to $p75^{NTR}$ and its co-receptors sortilin and NRH2, we found no modifications in expression levels of these proteins between clinical groups, which are similar to previous findings in the AD hippocampus (47, 48) and the MCI cortex (49). Sortilin and NHR2 are $p75^{NTR}$-binding partners, and blocking them precludes the binding of proNGF to $p75^{NTR}$ resulting in cell death (9, 10, 13, 50, 51). In this regard, increasing levels of proNGF and stable levels of $p75^{NTR}$/sortilin/NHR2 complexes may favor pro-apoptotic signaling in the hippocampus in AD. Interestingly, in vivo models indicate that proNGF is neurotoxic for aged but not young NGF-responsive basal forebrain neurons and that blockade of sortilin rescues proNGF induced cell death (47, 48). Together, these data suggest a molecular link in the brain between normal aging and AD through the regulation of proNGF and its cognate receptors and co-chaperones. In addition, increased proNGF levels also drive alterations in metabolic enzymes such as plasmin and matrix metalloprotease 9 (52), which regulate the maturation and degradation of mature NGF in the extracellular space and are decreased and increased, respectively, in parallel with the

accumulation of proNGF in MCI and AD brains (53). In fact, pharmacologically induced chronic failure in extracellular NGF maturation leads to mature NGF reduction, proNGF accumulation, cholinergic degeneration, and cognitive impairment in rats (54). In the present study, the observed negative correlation between hippocampal proNGF and cognitive function further demonstrates the importance of maintaining homeostatic regulation of the NGF neurotrophic system to cognition during the onset of AD.

Hippocampal TrkA, $p75^{NTR}$, Sortilin and NHR2 Levels During Disease Progression

We found a significant decrease in TrkA expression levels in the MCI hippocampus compared to NCI and AD, suggesting a return to control levels as subjects transition from MCI to AD. Reduction in TrkA in the face of stable proNGF may enhance binding between proNGF and the $p75^{NTR}$/sortilin/NRH2 complex, potentially shifting away from pro-survival signaling to pro-apoptotic signaling during prodromal AD. The unexpected rebound of TrkA levels in AD hippocampus to control levels indicates yet another example of the resilience of the human brain (4), perhaps in an attempt to stave off or slow the disease processes (7). It is important to note that NGF binding to TrkA reduces, whereas NGF binding to $p75^{NTR}$ activates β-secretase cleavage of the amyloid precursor protein (20, 21), providing a molecular link between neurotrophic signaling in normal brain aging and AD and amyloid processing. Early reduction in hippocampal TrkA may also exacerbate the toxic effects of the amyloid protein during the prodromal stage of AD. However, the increase in TrkA found in AD suggests yet another neuroplastic response to the disease process. In this regard, hippocampal CA1 neuronal TrkB expression is increased in cognitively intact cases displaying early-stage Braak I-II pathology compared with cognitively intact individuals with no NFTs (55). Although we did not find differences in any of the protein levels evaluated when we grouped our NCI cases into Braak stage I-II vs. Braak stage III and above, our cohort did not contain NCI pathology-free cases. Further studies are needed to compare cognitively intact individuals to those with no NFTs, plaques only or pathology-free cases. These observations further suggest that increased trophic factor activity marks brain reserve/resilience throughout the disease process.

We found stable amyloid protein levels in the hippocampus across disease stages, similar to the lack of expression level changes for amyloid precursor protein and its metabolites reported in hippocampal CA1 neurons in MCI and AD (56). However, the harsh treatments needed to extract amyloid for quantitation may contribute to this observation. By contrast, others reported increased $A\beta_{1\text{-}42}$ and $A\beta_{40/42}$ ratio in the hippocampus of severe AD Braak stage VI cases (57). The severity of NFT pathology in these cases compared to our cohort may explain this difference. Nevertheless, the precise role that amyloid plays, if any, in the activation of neurodegenerative events during the onset of AD awaits further characterization (58).

Hippocampal Akt and Erk Levels During Disease Progression

Several downstream kinase-signaling cascades have been identified in NGF/TrkA survival activation (59). We found in AD hippocampus a significant increase in the phospho-Akt to Akt ratio (60), but little difference among 3 clinical groups in their expression levels of hippocampal Erk, phospho-Erk. A recent quantitative immunohistochemical study found an increase in Erk2 pT185/187 in samples taken from the mid-hippocampus of AD compared to NCI cases (60), whereas the present tissue was obtained from the caudal hippocampus. Therefore, these discrepancies may relate to methodological or regional differences. Although the precise biological actions of an increase in phospho-Akt remains a challenging question in AD research, Akt may serve to suppress apoptosis directly by activating several different anti-apoptotic proteins, suppressing GSK3 apoptotic activities, or by blocking the function of the JNK pathway (61). Interestingly, in vivo findings also indicate that $p75^{NTR}$

can activate Akt via a phosphatidylinositol 3-kinase pathway which facilitates cell survival (62). These observations suggest that Akt mediates cell survival at a number of levels, depending upon target availability and the requirement for transcriptional or post-transcriptional events to suppress apoptosis.

Hippocampal JNK Levels During Disease Progression

Although proNGF upstream receptor binding initiates downstream JNK apoptotic signaling (63), we found that JNK remained stable across clinical groups. However, phospho-JNK and the ratio of phospho-JNK to JNK were significantly increased in AD compared to NCI and MCI. The increase in phospho-JNK may reflect a chronic and accumulative stress process that builds during the disease process and may be a very early marker for neuronal degeneration as it is associated with neurofibrillary alteration in some elderly controls (64). In the transition from MCI to AD, hippocampal phospho-JNK activation occurs in the face of increased levels of proNGF and phospho-Akt and reduced level of TrkA, despite no change in amyloid level. This suggests that increasing TrkA and phospho-Akt in AD might offset a shift toward JNK-mediated apoptotic signaling in AD. Similar to proNGF, we found that higher hippocampal phospho-JNK levels correlated with lower cognitive test scores, suggesting that pro-apoptotic signaling abnormalities ultimately override the putative compensatory TrkA-mediated pro-survival cascades as the disease progresses.

Neuropathological and Clinical Correlation with Hippocampal proNGF, Phospho-Akt, and Phospho-JNK during Disease Progression

When utilizing the Braak scores for NFT number and anatomic distribution and NIA-Reagan criteria for pathological diagnosis, combined with CERAD pathological findings, we found remarkable similarity in the degree of pathology between the MCI and AD groups, although only the AD group displayed an upregulation of hippocampal proNGF, phospho-Akt, and phospho-JNK activity. These data suggest that global AD-like pathology in general does not mediate the increase of these proteins. Of particular interest is the observation that many NCI cases displayed Braak, NIA-Reagan, and CERAD scores similar to that seen in both MCI and AD subjects; this was previously reported also in our other studies using RROS tissue (24, 65) as well as in other MCI populations (66, 67). Moreover, there was a positive correlation between TrkA and severity of pathology. Together the present findings suggest the need to rethink the involvement of classic AD pathology in the early initiation and/or generation of neurotrophic dysfunction in the early stages of AD. Moreover, the negative correlation between proNGF and cognitive function was observed both in the hippocampus and, previously, in the cortex (33). On the other hand, hippocampal TrkA levels did not correlate with cognitive function, whereas cortical TrkA levels were positively correlated with cognitive function (36). These findings suggest that alterations in NGF upstream and downstream signaling are associated with conversion to AD (68-70).

Summary

A schematic summary of the present study is presented in Figure 5. Whether alterations in proNGF signaling pathways are a primary event in the pathogenesis of AD or a secondary response to other pathological changes remain unknown. Because we found overlapping plaque and NFT pathology and no modification in the expression levels of $A\beta_{1\text{-}40}$, $A\beta_{1\text{-}42}$ and $A\beta_{40/42}$ ratio across clinical groups, these degenerative events may not play a direct role in hippocampal neurotrophin dysregulation. In the present study, the positive correlation observed between hippocampal proNGF and phospho-JNK levels, and their negative correlation with cognitive test scores including episodic memory, indicates that hippocampal NGF signaling abnormalities play a pervasive and key role in cognitive impairment during the onset of AD and represent drug targets for the treatment of dementia.

Acknowledgments

The authors declare that they have no conflict of interest. The authors thank the nuns, priests, and brothers from across the country that participated in the Religious Orders Study and Rush Alzheimer's Disease Center staff. The authors also thank patients and research participants at the University of Kentucky Alzheimer's Disease Center.

Supported by NIA Grants PO1AG14449, PO1AG9466 and P30AG10161.

REFERENCES

1. Apostolova LG, Hwang KS, Andrawis JP, et al. 3D PIB and CSF biomarker associations with hippocampal atrophy in ADNI subjects. Neurobiol Aging. 2010; 31:1284–303. [PubMed: 20538372]
2. Devanand DP, Pradhaban G, Liu X, et al. Hippocampal and entorhinal atrophy in mild cognitive impairment: prediction of Alzheimer disease. Neurology. 2007; 68:828–36. [PubMed: 17353470]
3. Ikonomovic MD, Mufson EJ, Wuu J, Cochran EJ, Bennett DA, DeKosky ST. Cholinergic plasticity in hippocampus of individuals with mild cognitive impairment: correlation with Alzheimer's neuropathology. J Alzheimers Dis. 2003; 5:39–48. [PubMed: 12590165]
4. DeKosky ST, Ikonomovic MD, Styren SD, et al. Upregulation of choline acetyltransferase activity in hippocampus and frontal cortex of elderly subjects with mild cognitive impairment. Ann Neurol. 2002; 51:145–55. [PubMed: 11835370]
5. Auld DS, Kornecook TJ, Bastianetto S, Quirion R. Alzheimer's disease and the basal forebrain cholinergic system: relations to beta-amyloid peptides, cognition, and treatment strategies. Prog Neurobiol. 2002; 68:209–45. [PubMed: 12450488]
6. Mufson EJ, Ginsberg SD, Ikonomovic MD, DeKosky ST. Human cholinergic basal forebrain: chemoanatomy and neurologic dysfunction. Journal of chemical neuroanatomy. 2003; 26:233–42. [PubMed: 14729126]
7. Mufson EJ, Binder L, Counts SE, et al. Mild cognitive impairment: pathology and mechanisms. Acta Neuropathol. 2012; 123:13–30. [PubMed: 22101321]
8. Fahnestock M, Yu G, Michalski B, et al. The nerve growth factor precursor proNGF exhibits neurotrophic activity but is less active than mature nerve growth factor. J Neurochem. 2004; 89:581–92. [PubMed: 15086515]
9. Kaplan DR, Miller FD. Neurobiology: a move to sort life from death. Nature. 2004; 427:798–9. [PubMed: 14985746]
10. Nykjaer A, Lee R, Teng KK, et al. Sortilin is essential for proNGF-induced neuronal cell death. Nature. 2004; 427:843–8. [PubMed: 14985763]
11. Mamidipudi V, Wooten MW. Dual role for p75(NTR) signaling in survival and cell death: can intracellular mediators provide an explanation? Journal of neuroscience research. 2002; 68:373–84. [PubMed: 11992464]
12. Teng KK, Hempstead BL. Neurotrophins and their receptors: signaling trios in complex biological systems. Cell Mol Life Sci. 2004; 61:35–48. [PubMed: 14704852]
13. Teng HK, Teng KK, Lee R, et al. ProBDNF induces neuronal apoptosis via activation of a receptor complex of p75NTR and sortilin. J Neurosci. 2005; 25:5455–63. [PubMed: 15930396]
14. Yoon SO, Casaccia-Bonnefil P, Carter B, Chao MV. Competitive signaling between TrkA and p75 nerve growth factor receptors determines cell survival. J Neurosci. 1998; 18:3273–81. [PubMed: 9547236]
15. Clewes O, Fahey MS, Tyler SJ, et al. Human ProNGF: biological effects and binding profiles at TrkA, P75NTR and sortilin. J Neurochem. 2008; 107:1124–35. [PubMed: 18808449]
16. Niewiadomska G, Mietelska-Porowska A, Mazurkiewicz M. The cholinergic system, nerve growth factor and the cytoskeleton. Behav Brain Res. 2011; 221:515–26. [PubMed: 20170684]
17. Song W, Volosin M, Cragnolini AB, Hempstead BL, Friedman WJ. ProNGF induces PTEN via p75NTR to suppress Trk-mediated survival signaling in brain neurons. J Neurosci. 2010; 30:15608–15. [PubMed: 21084616]

18. Vaegter CB, Jansen P, Fjorback AW, et al. Sortilin associates with Trk receptors to enhance anterograde transport and neurotrophin signaling. Nat Neurosci. 2011; 14:54–61. [PubMed: 21102451]
19. Kaplan DR, Miller FD. Neurotrophin signal transduction in the nervous system. Curr Opin Neurobiol. 2000; 10:381–91. [PubMed: 10851172]
20. Brann AB, Scott R, Neuberger Y, et al. Ceramide signaling downstream of the p75 neurotrophin receptor mediates the effects of nerve growth factor on outgrowth of cultured hippocampal neurons. J Neurosci. 1999; 19:8199–206. [PubMed: 10493721]
21. Costantini C, Weindruch R, Della Valle G, Puglielli L. A TrkA-to-p75NTR molecular switch activates amyloid beta-peptide generation during aging. Biochem J. 2005; 391:59–67. [PubMed: 15966860]
22. Griffin RJ, Moloney A, Kelliher M, et al. Activation of Akt/PKB, increased phosphorylation of Akt substrates and loss and altered distribution of Akt and PTEN are features of Alzheimer's disease pathology. J Neurochem. 2005; 93:105–17. [PubMed: 15773910]
23. Harrington AW, Kim JY, Yoon SO. Activation of Rac GTPase by p75 is necessary for c-jun N-terminal kinase-mediated apoptosis. J Neurosci. 2002; 22:156–66. [PubMed: 11756498]
24. Mufson EJ, Chen EY, Cochran EJ, Beckett LA, Bennett DA, Kordower JH. Entorhinal cortex beta-amyloid load in individuals with mild cognitive impairment. Exp Neurol. 1999; 158:469–90. [PubMed: 10415154]
25. Bennett DA, Schneider JA, Arvanitakis Z, Kelly JF, Aggarwal NT, Shah RC, Wilson RS. Neuropathology of older persons without cognitive impairment from two community-based studies. Neurology. 2006; 66:1837–44. [PubMed: 16801647]
26. Bennett DA, Schneider JA, Bienias JL, Evans DA, Wilson RS. Mild cognitive impairment is related to Alzheimer disease pathology and cerebral infarctions. Neurology. 2005; 64:834–41. [PubMed: 15753419]
27. Perez SE, Getova DP, He B, et al. Rac1b increases with progressive tau pathology within cholinergic nucleus basalis neurons in Alzheimer's disease. The American journal of pathology. 2012; 180:526–40. [PubMed: 22142809]
28. Schmitt FA, Davis DG, Wekstein DR, et al. "Preclinical" AD revisited: neuropathology of cognitively normal older adults. Neurology. 2000; 55:370–6. [PubMed: 10932270]
29. Braak H, Braak E. Neuropathological stageing of Alzheimer-related changes. Acta Neuropathol. 1991; 82:239–59. [PubMed: 1759558]
30. Newell KL, Hyman BT, Growdon JH, Hedley-Whyte ET. Application of the National Institute on Aging (NIA)-Reagan Institute criteria for the neuropathological diagnosis of Alzheimer disease. J Neuropathol Exp Neurol. 1999; 58:1147–55. [PubMed: 10560657]
31. Mirra SS. The CERAD neuropathology protocol and consensus recommendations for the postmortem diagnosis of Alzheimer's disease: a commentary. Neurobiol Aging. 1997; 18:S91–4. [PubMed: 9330994]
32. Counts SE, Nadeem M, Wuu J, Ginsberg SD, Saragovi HU, Mufson EJ. Reduction of cortical TrkA but not p75(NTR) protein in early-stage Alzheimer's disease. Ann Neurol. 2004; 56:520–31. [PubMed: 15455399]
33. Peng S, Wuu J, Mufson EJ, Fahnestock M. Increased proNGF levels in subjects with mild cognitive impairment and mild Alzheimer disease. J Neuropathol Exp Neurol. 2004; 63:641–9. [PubMed: 15217092]
34. Davis AA, Fritz JJ, Wess J, Lah JJ, Levey AI. Deletion of M1 muscarinic acetylcholine receptors increases amyloid pathology in vitro and in vivo. J Neurosci. 2010; 30:4190–6. [PubMed: 20335454]
35. Counts SE, He B, Nadeem M, Wuu J, Scheff SW, Mufson EJ. Hippocampal drebrin loss in mild cognitive impairment. Neuro-degenerative diseases. 2012; 10:216–9. [PubMed: 22310934]
36. Counts SE, Nadeem M, Wuu J, Ginsberg SD, Saragovi HU, Mufson EJ. Reduction of cortical TrkA but not p75(NTR) protein in early-stage Alzheimer's disease. Ann Neurol. 2004; 56:520–31. [PubMed: 15455399]

37. Ginsberg SD, Mufson EJ, Counts SE, et al. Regional selectivity of rab5 and rab7 protein upregulation in mild cognitive impairment and Alzheimer's disease. J Alzheimers Dis. 2010; 22:631–9. [PubMed: 20847427]
38. Nieto A, Montejo de Garcini E, Avila J. Altered levels of microtubule proteins in brains of Alzheimer's disease patients. Acta Neuropathol. 1989; 78:47–51. [PubMed: 2735189]
39. Sze CI, Bi H, Kleinschmidt-DeMasters BK, Filley CM, Martin LJ. Selective regional loss of exocytotic presynaptic vesicle proteins in Alzheimer's disease brains. J Neurol Sci. 2000; 175:81–90. [PubMed: 10831767]
40. Armitage, P.; Berry, G.; Matthews, JNS. Statistical Methods in Medical Research. 4th ed. Blackwell Science Ltd.; Oxford: 2002.
41. Kleinbaum, DG.; Kupper, LL.; Muller, KE.; Nizam, A. Applied Regression Analysis and Other Multivariable Methods. 3rd edition. Duxbury Press; Pacific Grove: 1998.
42. Johnson, RA.; Wichern, DW. Applied Multivariate Statistical Analysis. 4th ed. Prentice Hall; Englewood Cliffs: 1998.
43. Murase K, Nabeshima T, Robitaille Y, Quirion R, Ogawa M, Hayashi K. NGF level of is not decreased in the serum, brain-spinal fluid, hippocampus, or parietal cortex of individuals with Alzheimer's disease. Biochemical and biophysical research communications. 1993; 193:198–203. [PubMed: 8503908]
44. Mufson EJ, Ikonomovic MD, Styren SD, et al. Preservation of brain nerve growth factor in mild cognitive impairment and Alzheimer disease. Arch Neurol. 2003; 60:1143–8. [PubMed: 12925373]
45. Pedraza CE, Podlesniy P, Vidal N, et al. Pro-NGF isolated from the human brain affected by Alzheimer's disease induces neuronal apoptosis mediated by p75NTR. Am J Pathol. 2005; 166:533–43. [PubMed: 15681836]
46. Podlesniy P, Kichev A, Pedraza C, et al. Pro-NGF from Alzheimer's disease and normal human brain displays distinctive abilities to induce processing and nuclear translocation of intracellular domain of p75NTR and apoptosis. Am J Pathol. 2006; 169:119–31. [PubMed: 16816366]
47. Al-Shawi R, Hafner A, Chun S, et al. ProNGF, sortilin, and age-related neurodegeneration. Ann N Y Acad Sci. 2007; 1119:208–15. [PubMed: 18056969]
48. Al-Shawi R, Hafner A, Olsen J, Chun S, Raza S, Thrasivoulou C, Lovestone S, Killick R, Simons P, Cowen T. Neurotoxic and neurotrophic roles of proNGF and the receptor sortilin in the adult and ageing nervous system. Eur J Neurosci. 2008; 27:2103–14. [PubMed: 18412630]
49. Mufson EJ, Wuu J, Counts SE, Nykjaer A. Preservation of cortical sortilin protein levels in MCI and Alzheimer's disease. Neuroscience letters. 2010; 471:129–33. [PubMed: 20085800]
50. Bronfman FC, Fainzilber M. Multi-tasking by the p75 neurotrophin receptor: sortilin things out? EMBO Rep. 2004; 5:867–71. [PubMed: 15470383]
51. Kim T, Hempstead BL. NRH2 is a trafficking switch to regulate sortilin localization and permit proneurotrophin-induced cell death. Embo J. 2009; 28:1612–23. [PubMed: 19407813]
52. Bruno MA, Cuello AC. Activity-dependent release of precursor nerve growth factor, conversion to mature nerve growth factor, and its degradation by a protease cascade. Proc Natl Acad Sci U S A. 2006; 103:6735–40. [PubMed: 16618925]
53. Bruno MA, Mufson EJ, Wuu J, Cuello AC. Increased matrix metalloproteinase 9 activity in mild cognitive impairment. J Neuropathol Exp Neurol. 2009; 68:1309–18. [PubMed: 19915485]
54. Allard S, Leon WC, Pakavathkumar P, Bruno MA, Ribeiro-da-Silva A, Cuello AC. Impact of the NGF maturation and degradation pathway on the cortical cholinergic system phenotype. J Neurosci. 2012; 32:2002–12. [PubMed: 22323714]
55. Kao PF, Banigan MG, Vanderburg CR, et al. Increased expression of TrkB and Capzb2 accompanies preserved cognitive status in early alzheimer disease pathology. J Neuropathol Exp Neurol. 2012; 71:654–64. [PubMed: 22710966]
56. Ginsberg SD, Alldred MJ, Counts SE, et al. Microarray analysis of hippocampal CA1 neurons implicates early endosomal dysfunction during Alzheimer's disease progression. Biol Psychiatry. 2010; 68:885–93. [PubMed: 20655510]

57. Aoki M, Volkmann I, Tjernberg LO, Winblad B, Bogdanovic N. Amyloid beta-peptide levels in laser capture microdissected cornu ammonis 1 pyramidal neurons of Alzheimer's brain. Neuroreport. 2008; 19:1085–9. [PubMed: 18596605]
58. Ikonomovic MD, Klunk WE, Abrahamson EE, et al. Precuneus amyloid burden is associated with reduced cholinergic activity in Alzheimer disease. Neurology. 2011; 77:39–47. [PubMed: 21700583]
59. Brunet A, Park J, Tran H, Hu LS, Hemmings BA, Greenberg ME. Protein kinase SGK mediates survival signals by phosphorylating the forkhead transcription factor FKHRL1 (FOXO3a). Mol Cell Biol. 2001; 21:952–65. [PubMed: 11154281]
60. Talbot K, Wang HY, Kazi H, et al. Demonstrated brain insulin resistance in Alzheimer's disease patients is associated with IGF-1 resistance, IRS-1 dysregulation, and cognitive decline. The Journal of clinical investigation. 2012; 122:1316–38. [PubMed: 22476197]
61. Song G, Ouyang G, Bao S. The activation of Akt/PKB signaling pathway and cell survival. J Cell Mol Med. 2005; 9:59–71. [PubMed: 15784165]
62. Roux PP, Barker PA. Neurotrophin signaling through the p75 neurotrophin receptor. Prog Neurobiol. 2002; 67:203–33. [PubMed: 12169297]
63. Mufson EJ, Counts SE, Perez SE, Ginsberg SD. Cholinergic system during the progression of Alzheimer's disease: therapeutic implications. Ex Rev Neurother. 2008; 8:1703–18.
64. Zhu X, Castellani RJ, Takeda A, et al. Differential activation of neuronal ERK, JNK/SAPK and p38 in Alzheimer disease: the 'two hit' hypothesis. Mechanisms of ageing and development. 2001; 123:39–46. [PubMed: 11640950]
65. Vana L, Kanaan NM, Ugwu IC, Wuu J, Mufson EJ, Binder LI. Progression of tau pathology in cholinergic Basal forebrain neurons in mild cognitive impairment and Alzheimer's disease. Ame J Pathol. 2011; 179:2533–50.
66. Petersen RC, Parisi JE, Dickson DW, et al. Neuropathologic features of amnestic mild cognitive impairment. Arch Neurol. 2006; 63:665–72. [PubMed: 16682536]
67. Price JL, McKeel DW Jr. Buckles VD, et al. Neuropathology of nondemented aging: presumptive evidence for preclinical Alzheimer disease. Neurobiol Aging. 2009; 30:1026–36. [PubMed: 19376612]
68. Aggarwal NT, Wilson RS, Beck TL, Bienias JL, Bennett DA. Mild cognitive impairment in different functional domains and incident Alzheimer's disease. J Neurology, Neurosurg Psychiatry. 2005; 76:1479–84.
69. Grober E, Hall CB, Lipton RB, Zonderman AB, Resnick SM, Kawas C. Memory impairment, executive dysfunction, and intellectual decline in preclinical Alzheimer's disease. J Int Neuropsychol Soc. 2008; 14:266–78. [PubMed: 18282324]
70. Mormino EC, Kluth JT, Madison CM, et al. Episodic memory loss is related to hippocampal-mediated beta-amyloid deposition in elderly subjects. Brain. 2009; 132:1310–23. [PubMed: 19042931]

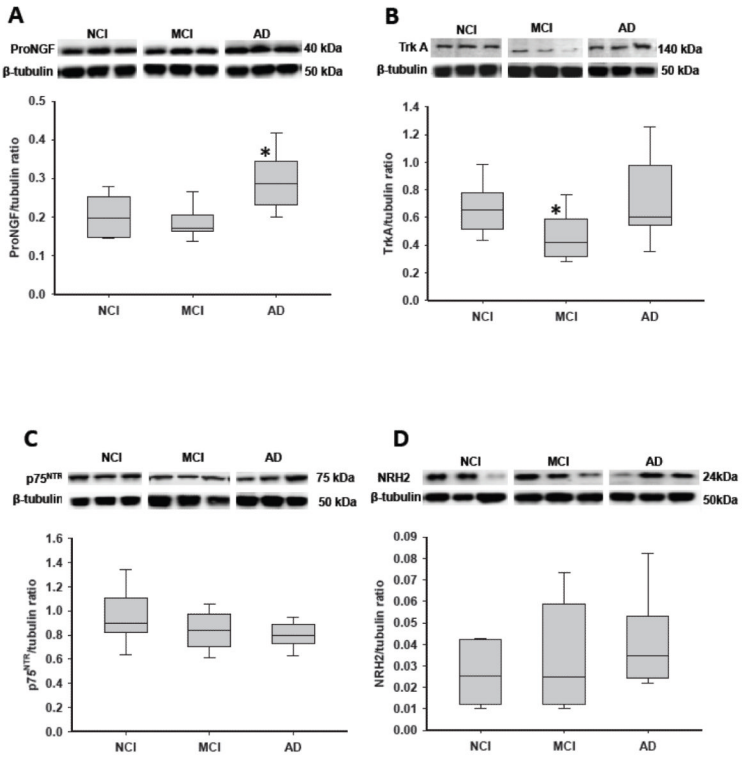

Figure 1.

Boxplots and representative immunoblots of hippocampal levels of precursor of nerve growth factor (ProNGF), TrkA, p75 neurotrophin receptor ($p75^{NTR}$) and neurotrophin receptor homolog-2 (NRH2) in cases clinically diagnosed as no cognitive impairment (NCI), mild cognitive impairment (MCI), and Alzheimer disease (AD). Immunoreactive signals were normalized to β-tubulin levels on the same blots by densitometry. (**A**) Levels of proNGF were significantly elevated in AD vs. NCI and MCI. *, p = 0.004. (**B**) Levels of TrkA were significantly reduced in MCI and upregulated in AD. *, p = 0.014. (**C, D**) Levels of $p75^{NTR}$ (**C**) and NRH2 (**D**) remained stable across clinical diagnoses.

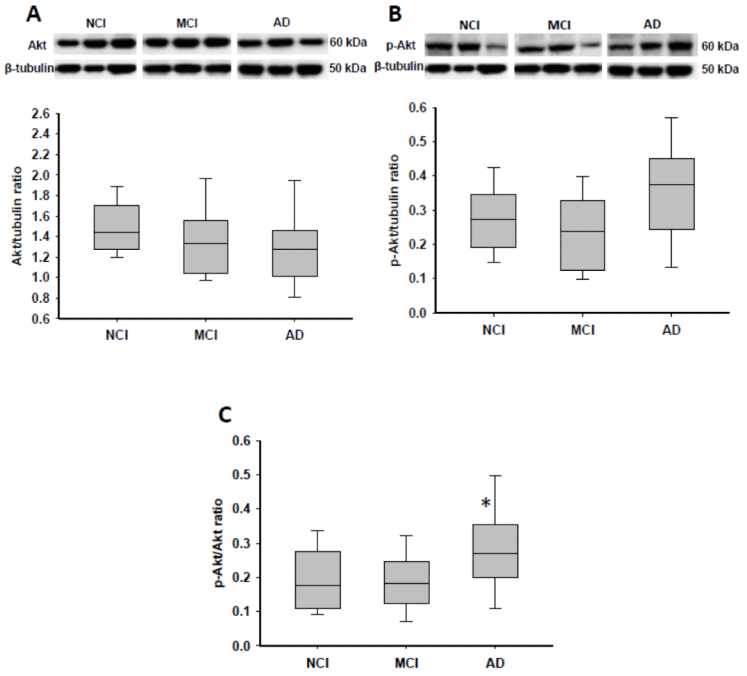

Figure 2.

Boxplots of hippocampal levels of Akt, phospho-Akt (p-Akt), and the ratio of p-Akt to Akt in cases clinically diagnosed as no cognitive impairment (NCI), mild cognitive impairment (MCI), and Alzheimer disease (AD). Representative immunoblots for p-Akt and Akt are also presented. (**A**) Levels of total Akt slightly decreased from NCI to MCI to AD. (**B**) Levels of p-Akt were increased in AD vs. NCI and MCI, but the difference did not reach statistical significance. (**C**) The p-Akt to Akt ratio was significantly higher in AD vs. NCI and MCI. *, p = 0.036.

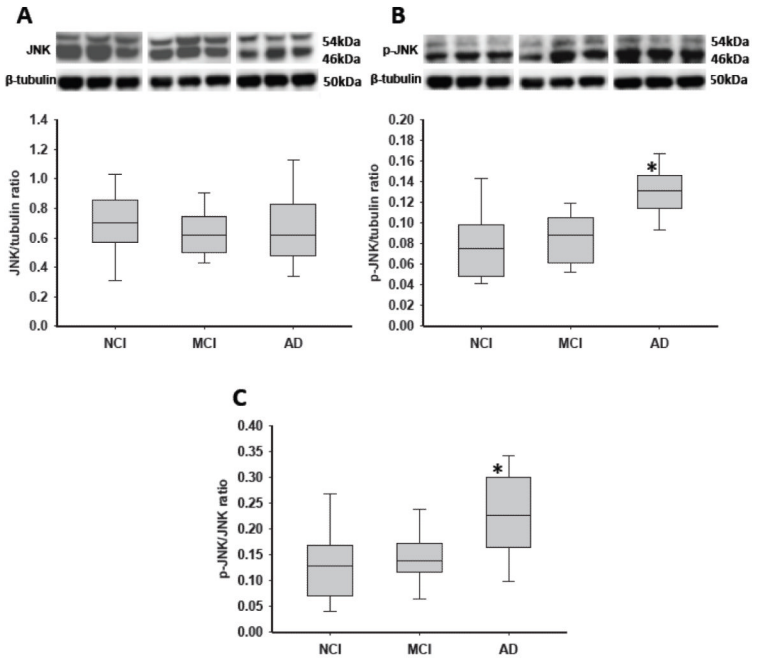

Figure 3.

Boxplots of hippocampal levels of c-jun kinase (JNK), phospho-JNK, and the ratio of phospho-JNK to JNK in cases clinically diagnosed as no cognitive impairment (NCI), mild cognitive impairment (MCI), and Alzheimer disease (AD). Representative immunoblots for phospho-JNK and JNK are also presented. (**A)** Levels of total JNK remained stable across clinical diagnosis. (**B)** Levels of phospho-JNK were significantly increased in AD vs. NCI and MCI. *, p = 0.0006. (**C**) Similar to phospho-JNK, the phospho-JNK to JNK ratio also showed significantly elevated levels in AD vs. MCI and NCI. *, p = 0.016.

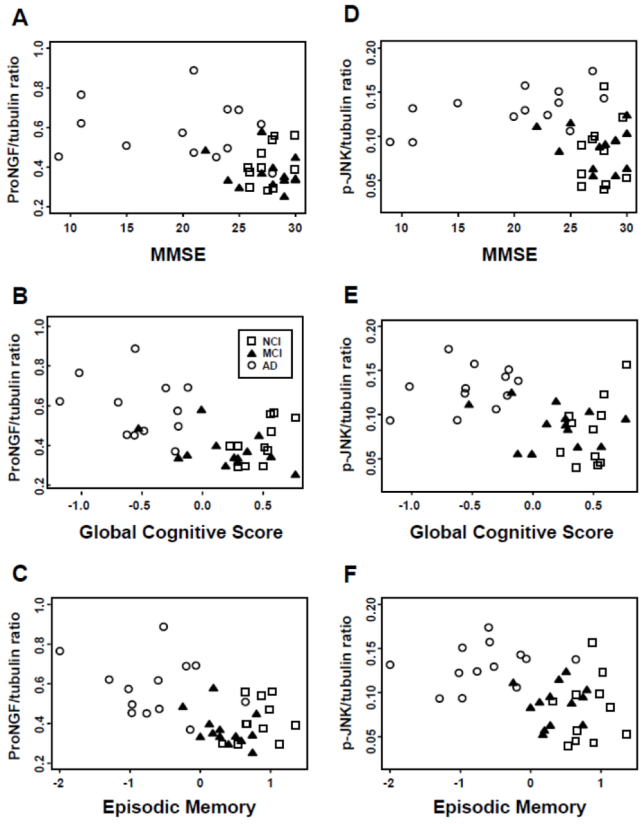

Figure 4.

(**A-F**) Hippocampal precursor of nerve growth factor (proNGF) and phospho-c-jun kinase (JNK) protein levels negatively correlated with cognitive function as measured by Mini-Mental State Examination (MMSE) (**A, D**), Global Cognitive Score (**B, E**), and episodic memory z-score (**C, F**). No cognitive impairment (NCI) = open squares; mild cognitive impairment (MCI) = filled triangles; Alzheimer disease (AD) = open circles.

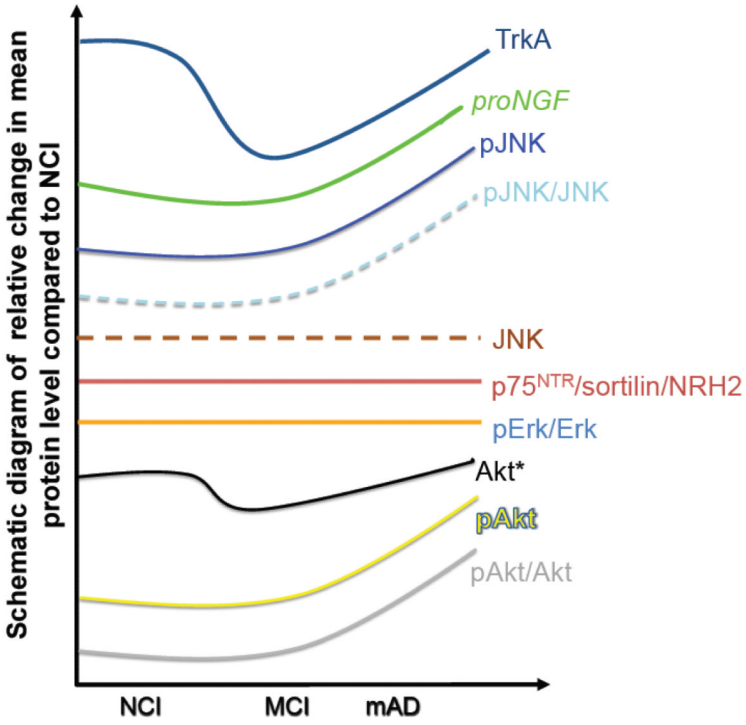

Figure 5.

Schematic summary diagram showing the relative changes for precursor of nerve growth factor (ProNGF), TrkA, p75 neurotrophin receptor ($p75^{NTR}$), neurotrophin receptor homolog-2 (NRH2), Erk, Akt, phospho-Akt, c-jun kinase (JNK) and phospho-JNK in the hippocampus during the progression of Alzheimer disease. No cognitive impairment (NCI); mild cognitive impairment (MCI); mild Alzheimer disease (mAD).

J Neuropathol Exp Neurol. Author manuscript; available in PMC 2013 November 01.

Table 1

Rush Religious Order Study Clinical, Demographic, and Neuropathological Characteristics by Diagnosis Category

		Clinical Diagnosis					
		NCI (n=11)	**MCI* (n=13)**	**AD (n=13)**	**Total (n=37)**	**p value**	**Pair-wise comparison**
Age (y) at death:	Mean ± SD (Range)	83.4 ± 4.6 (76-93)	85.4 ± 4.0 (79-92)	87.7 ± 5.8 (76-98)	85.6 ± 5.1 (76-98)	0.1[a]	--
Number (%) of males:		5 (45%)	5 (38%)	6 (46%)	16 (43%)	1.0[b]	--
Years of education:	Mean ± SD (Range)	17.5 ± 4.7 (10-25)	17.7 ± 3.8 (10-25)	19.0 ± 3.3 (14-26)	18.1 ± 3.9 (10-26)	0.8[a]	--
Number (%) with ApoE ε4 allele:		0	5 (38%)	4 (31%)	9 (24%)	0.058[b]	--
MMSE:	Mean ± SD (Range)	27.6 ± 1.4 (26-30)	27.5 ± 2.5 (22-30)	19.9 ± 6.4 (9-28)	24.9 ± 5.5 (9-30)	0.0002[a]	(NCI, MCI) > AD
Global Cognitive Score:	Mean ± SD (Range)	0.5 ± 0.2 (0.2-0.8)	0.2 ± 0.3 (−0.5, 0.8)	−0.5 ± 0.3 (−1.2, −0.1)	0.0 ± 0.5 (−1.2, 0.8)	<0.0001[a]	NCI > MCI > AD
Episodic Memory *Z*-score:	Mean ± SD (Range)	0.8 ± 0.3 (0.3, 1.4)	0.4 ± 0.3 (−0.2, 0.8)	−0.6 ± 0.7 (−2.0, 0.6)	0.1 ± 0.8 (−2.0, 1.4)	<0.0001[a]	NCI > MCI > AD
Post-mortem interval (hours):	Mean ± SD (Range)	5.7 ± 3.3 (1.0-12.4)	5.6 ± 2.5 (2.0-10.6)	4.2 ± 1.6 (1.5-7.3)	5.1 ± 2.5 (1.0-12.4)	0.4[a]	--
Distribution of Braak scores:	I/II	4	2	1	7		
	III/IV	6	8	8	22	0.14[a]	--
	V/VI	1	3	4	8		
NIA Reagan diagnosis (likelihood of AD):	No AD	0	0	0	0		
	Low	6	5	1	12	0.042[a]	NCI < AD
	Intermediate	5	5	9	19		
	High	0	3	0	6		
CERAD diagnosis:	No AD	3	4	0	7		
	Possible	2	0	0	2	0.0076[a]	NCI < AD
	Probable	6	6	7	19		
	Definite	0	3	6	9		

AD = Alzheimer disease; CERAD = Consortium to Establish a Registry for Alzheimer Disease; MCI = mild cognitive impairment; MMSE = Mini-Mental State Examination; NCI = no cognitive impairment.

*4 of the 13 MCI cases were amnestic MCI.

[a] Kruskal-Wallis test, with Bonferroni correction for multiple comparisons.

[b] Fisher's exact test, with Bonferroni correction for multiple comparisons.

Table 2

Antibodies

	Antibodies	Epitope or Immunogen	Dilution	Company and Catalog #
proNGF	rabbit polyclonal to NGF (H-20)	N-terminus of NGF	1:50	Santa Cruz Biotechnology; Santa Cruz, CA # sc-548
TrkA receptor	rabbit polyclonal to TrkA	External domain of TrkA	1:100	Fitzgerald Industries International, Acton, MA # 20R-TR013
$p75^{NTR}$ receptor	rabbit polyclonal to p75 NGF receptor	aa' 250-350 of $p75^{NTR}$	1:500	Abcam; Cambridge, MA # ab38335
Sortilin	rabbit polyclonal to Sortilin	C-terminus of sortilin	1:1000	Abcam; # ab16640
NHR2	rabbit polyclonal to NHR2	N-terminus of NHR2 (discontinued)	1:1000	Abcam; # ab18460 (discontinued)
Akt	rabbit polyclonal to Akt	C-terminus of Akt	1:1000	Cell Signaling Technology, Danvers, MA # 9272
phospho-Akt	rabbit polyclonal to phospho-Akt	phospho-Ser 473	1:1000	Cell Signaling Technology; # 9271
JNK	rabbit polyclonal to SAPK/JNK (56G8)	Human JUNK2/MBP	1:1000	Cell Signaling Technology; # 9258
phospho-JNK	rabbit polyclonal to phospho SAPK/JNK (81E11)	phospho-Thr 183, Phospho-Tyr 185	1:2000	Cell Signaling Technology; # 4668
Erk	rabbit polyclonal to p44/42 MAPK (Erk1/2)	Erk1 (p44), Erk2 (p42)	1:1000	Cell Signaling Technology; #9102
phospho-Erk	mouse monoclonal to phospho p44/42 MAPK (Erk1/2) (E10 clone)	phospho-Thr202, phospho-Tyr204	1:2000	Cell Signaling Technology; #9106
β-tubulin	mouse monoclonal to (KMX-1 clone)	tubulin from polycephalum myxamoebae	1:4000	Millipore, Billerica, MA # MAB3408

proNGF, precursor of nerve growth factor (ProNGF); $p75^{NTR}$, p75 neurotrophin receptor; NRH2, neurotrophin receptor homolog-

Table 3

Summary of Hippocampal Protein Levels by Diagnosis Category

	Clinical Diagnosis					
	NCI (N=11)	**MCI (N=13)**	**AD (N=13)**	**Total (N=37)**	**P-value***	**Pair-wise comparison***
ProNGF	0.41 ± 0.10 (0.29-0.56)	0.37 ± 0.09 (0.25-0.58)	0.58 ± 0.15 (0.37-0.88)	0.46 ± 0.15 (0.25-0.88)	0.004	(NCI, MCI) < AD
TrkA	0.64 ± 0.15 (0.43-0.91)	0.47 ± 0.17 (0.27-0.89)	0.74 ± 0.31 (0.25-1.32)	0.62 ± 0.25 (0.25-1.32)	0.014	(NCI, AD) > MCI
Phospho-Erk	0.08 ± 0.02 (0.04-0.10)	0.10 ± 0.05 (0.02-0.22)	0.09 ± 0.05 (0.03-0.18)	0.09 ± 0.04 (0.02-0.22)	0.6	--
Erk	0.82 ± 0.22 (0.32-1.11)	0.86 ± 0.29 (0.38-1.36)	0.90 ± 0.25 (0.48-1.35)	0.86 ± 0.25 (0.32-1.36)	0.7	--
Erk ratio	0.10 ± 0.03 (0.05-0.15)	0.13 ± 0.10 (0.04-0.33)	0.10 ± 0.04 (0.04-0.16)	0.11 ± 0.07 (0.04-0.33)	0.9	--
Phospho-Akt	0.28 ± 0.10 (0.13-0.50)	0.26 ± 0.09 (0.12-0.42)	0.36 ± 0.13 (0.16-0.57)	0.30 ± 0.11 (0.12-0.57)	0.1	--
Akt	1.46 ± 0.22 (1.18-2.00)	1.37 ± 0.38 (1.00-2.36)	1.29 ± 0.39 (0.78-2.27)	1.37 ± 0.34 (0.78-2.36)	0.3	--
Akt ratio	0.20 ± 0.08 (0.09-0.38)	0.20 ± 0.08 (0.07-0.40)	0.29 ± 0.12 (0.13-0.58)	0.23 ± 0.10 (0.07-0.58)	0.036	MCI < AD
p75	0.94 ± 0.23 (0.55-1.44)	0.84 ± 0.16 (0.55-1.10)	0.79 ± 0.11 (0.62-0.96)	0.85 ± 0.18 (0.55-1.44)	0.2	--
Sortilin	3.32 ± 1.72 (1.30-5.63)	2.76 ± 1.03 (0.99-5.09)	3.23 ± 1.56 (0.93-6.39)	3.09 ± 1.43 (0.93-6.39)	0.8	--
NRH2**	0.07 ± 0.06 (0.02-0.23)	0.08 ± 0.06 (0.02-0.19)	0.08 ± 0.05 (0.04-0.21)	0.07 ± 0.06 (0.02-0.23)	0.5	--
Phospho-JNK	0.08 ± 0.04 (0.04-0.16)	0.09 ± 0.02 (0.05-0.12)	0.13 ± 0.02 (0.09-0.17)	0.10 ± 0.04 (0.04-0.17)	0.0006	(NCI, MCI) < AD
JNK	0.72 ± 0.24 (0.17-1.08)	0.64 ± 0.16 (0.41-0.98)	0.66 ± 0.26 (0.28-1.22)	0.67 ± 0.22 (0.17-1.22)	0.5	--
JNK ratio	0.13 ± 0.08 (0.04-0.27)	0.15 ± 0.05 (0.06-0.25)	0.22 ± 0.08 (0.09-0.35)	0.17 ± 0.08 (0.04-0.35)	0.016	(NCI, MCI) < AD

Data are expressed as mean ± SD (range).

NCI = no cognitive impairment; MCI = mild cognitive impairment; AD = Alzheimer disease; proNGF = precursor form of nerve growth factor; JNK = c-jun kinase.

*Kruskal-Wallis test, with Bonferroni correction for multiple comparisons.

**NRH2 data was obtained from a subset of ROS cases (5 NCI, 4 MCI, 4 AD) and additional UKADC cases (7 NCI, 5 MCI, 3 AD).

Table 4

Summary of Hippocampal Amyloid Load by Diagnosis Category

	Clinical Diagnosis				
	NCI (N=11)	**MCI (N=13)**	**AD (N=13)**	**Total (N=37)**	**P-value**
SDS 42	8.39 ± 1.13 (6.55-9.88)	9.27 ± 1.11 (6.71-11.49)	9.00 ± 0.82 (7.82-10.29)	8.94 ± 1.04 (6.55-11.49)	0.1
SDS 40	5.43 ± 0.80 (4.73-7.59)[a]	5.36 ± 0.58 (4.37-6.43)	5.45 ± 0.43 (4.73-6.16)	5.43 ± 0.62 (4.37-7.59)	0.7
SDS42/40 ratio	*2.96 ± 1.34 (0.17-4.24)*[b]	*3.92 ± 1.05 (1.60-5.71)*	*3.55 ± 0.71 (2.43-4.75)*	*3.51 ± 1.08 (0.17-5.71)*	*0.2*
FA 42	9.13 ± 1.33 (7.20-11.17)	8.43 ± 2.33 (4.23-12.31)	9.03 ± 1.68 (5.96-10.59)	8.96 ± 1.80 (4.23-12.31)	0.6
FA 40	6.30 ± 0.75 (5.44-8.02)	6.18 ± 1.12 (4.86-9.04)	6.19 ± 0.93 (4.75-7.92)	6.29 ± 0.99 (4.75-9.04)	0.6
FA 42/40 ratio	*2.83 ± 1.56 (−0.82, 4.85)*	*2.25 ± 1.69 (−1.52, 4.29)*	*2.92 ± 1.24 (1.07-4.75)*	*2.66 ± 1.48 (−1.52, 4.85)*	*0.5*

Mean ± SD (range).

SDS = sodium dodecyl sulfate-soluble fractions; FA = formic acid fractions.

[*] All values were log-transformed so these summary statistics were less skewed by the non-normality in the data.

[a] After exclusion of one outlier: 5.21 ± 0.38 (4.73-5.88).

[b] After exclusion of one outlier: 3.24 ± 1.02 (1.34-4.24).